Supporting Information

Metal-Organic Frameworks/Conducting Polymer Hydrogel Integrated 3D Free-Standing Monoliths as Ultrahigh Loading Li–S Battery Electrodes

Borui Liu,[†] Renheng Bo,[†] Mahdiar Taheri,[‡] Iolanda Di Bernardo,[†] Nunzio Motta,[⁄⁄] Hongjun Chen,[†] Takuya Tsuzuki,[‡] Guihua Yu,[§] and Antonio Tricoli[†]*

[†] Nanotechnology Research Laboratory, Research School of Electrical, Energy and Materials Engineering, Australian National University, Canberra, ACT 2601, Australia.

[‡] Laboratory of Advanced Nanomaterials for Sustainability, Research School of Electrical, Energy and Materials Engineering, Australian National University, Canberra, ACT 2601, Australia.

[§] Materials Science and Engineering Program and Department of Mechanical Engineering, The University of Texas at Austin, Austin, Texas 78712, USA.

[⁄⁄] School of Chemistry, Physics and Mechanical Engineering, Queensland University of Technology, Brisbane, QLD 4001, Australia.

Fabrication of SuperP@PANi CPH/MF

The PANi precursor solutions are prepared using on a modified strategy of literature[S1] and our previous related works.[S2, S3] First of all, 2.86 g (12.5 mmol) ammonium persulfate was dissolved in 10 mL de-ionized (DI) water to form solution A. Then, 9.21 mL (10 mmol) phytic acid (50%, wt. in water, Sigma Aldrich), 4.58 mL (50 mmol) aniline and 20 mL DI water are thoroughly mixed together to form solution B. A certain amount of SuperP (SP) carbon black nanoparticles of about 4 g are added into solution B and stirred overnight to create a homogenous solution C. The melamine foam (MF) is diced into small cubes (side length: ca. 2 to 3 cm) and cleaned by ethanol and dried in a vacuum oven at 60 °C for 12 hours before further use. Afterwards, a MF cube is soaked in the mixture of solution A and solution C (cooled to 4 °C in ice-water bath) with repeated squeezing for about 5 min to allow the SP@PANi CPH to completely fill in the MF porous cube. Then, wait for 6 hours for a complete gelation of the PANi hydrogel. References are superscripted and appear after the punctuation.

Purification and dehydration of SP@PANi CPH/MF

The SP@PANi CPH/MF cube is purified by immersing in DI water for 24 hours, followed by freeze-drying for 48 hours. The dried SP@PANi CPH/MF cube is further diced into flat round discs (d = 15 mm). The SP@PANi CPH/MF discs could be easily re-sized into other necessary dimensions in accordance with demands by simply changing the dicing molds.

Fabrication of N,P co-doped 3D CIMC current collectors

The SP@PANi CPH/MF discs are collected and pyrolyzed in a tube furnace at 1000 °C for 3 hours under Ar flow protection. The temperature ramping speed is 3 °C min^{-1}. During the pyrolysis process, SP@PANi CPH/MF discs are mechanically sandwiched between two pieces of quartz slices in order to keep the planar shape of the discs unchanged. Afterwards, the as-prepared N,P co-doped 3D CIMC current collectors are rinsed with DI water and isopropyl alcohol (IPA) mixture (1:1, vol.) and dried in a vacuum oven at 60 °C overnight before further use.

Fabrication of 3D ZIF67-CIMC and 3D HKUST1-CIMC current collectors

The mass percentage of MOF nanoparticles in 3D CIMC can be easily determined by thermogravimetric analysis (TGA) and the weight difference before and after MOF synthesis process. Prior to the synthesis of 3D ZIF67-CIMC and 3D HKUST1-CIMC current collectors, CIMC current collectors are treated with 8 M nitric acid for 2 hours under low vacuum, followed by immersing in DI water and dried in a vacuum oven overnight. To synthesize the 3D ZIF67-CIMC current collectors, 0.5 mmol cobalt acetate tetrahydrate and 8 mmol 2-methylimidazole are dissolved in 10 mL methanol separately. CIMC current collector is hanged in the ligand solution for 30 min while stirring, then the metal source solution is added to that. After 18 hours of stirring at room temperature, the 3D CIMC current collector is collected and rinsed with methanol three times and dried in a vacuum oven at 60 °C overnight. To synthesize the 3D HKUST1-CIMC current collectors, 1.5 mmol copper acetate monohydrate is dissolved in 10 mL water and 1 mmol 1,3,5-benzenetricarboxylic acid is dissolved 10mL ethanol.

Then, similar procedures to that described for 3D ZIF67-CIMC current collectors are followed.

Fabrication of S/3D CIMC, S/3D ZIF67-CIMC, and S/3D HKUST1-CIMC electrodes

A certain amount of sulfur powder, in accordance with demands, is weighed and mixed with the 3D current collectors and heat-treated at 155 °C for 12 hours in a well-sealed glass container. The mass loading of sulfur in the 3D current collector were determined by the weight difference before and after sulfur impregnation.

Materials Characterizations

Crystallographic phases of the 3D CIMC, 3D ZIF67-CIMC and 3D HKUST1-CIMC samples are determined by a Bruker system (XRD, D2 Phaser, USA) equipped with Cu Kα radiation of average wavelength 1.54059 Å. The morphologies of the materials are characterized by scanning electron microscope (SEM, Zeiss UltraPlus FESEM) at 3 kV and transmission electron microscope (TEM, JEOL 2100F FEGTEM) at 200 kV. Energy dispersive X-ray (EDX) elemental mapping is performed with Zeiss UltraPlus FESEM. TGA is carried out with a NETZSCH STA 449 F3 Jupiter analyzing instrument. Digital images are taken with an iPhone 7 Plus camera. The cycled electrodes are soaked in a mixture of DME and DOL (1:1, vol./vol.) for 30 min to remove most of the impurities and then naturally dried and examined under SEM. Nitrogen adsorption isotherms of the degassed specimens are recorded at liquid nitrogen temperature using a Tristar II (Micromeritics, USA). Langmuir and Brunauer–Emmett–Teller models are

applied to determine the specific surface area of all samples in the pressure range between 0.23 and 60 mmHg for Langmuir model, and p/p0 between 0.001 and 0.05 for BET model. UV-vis absorption spectroscopy is performed with a Cary 60 UV-vis (Agilent Technologies) to compare the contents of LiPS species from the DOL/DME (10mL, 1:1, vol.)-soaked post-cycling electrodes. Typically, the electrodes are soaked in DOL/DME mixture for 60 min. X-ray photoemission spectroscopy (XPS) data are collected in a Thermofisher Kratos Axis Supra photoelectron spectrometer at the Central Analytical Research Facility of the Queensland University of Technology (Brisbane, Australia). The apparatus is equipped with a monochromated Al k_α source (1486.7 eV), and the spectra were calibrated with respect to the substrate signal. Survey spectra were acquired at pass energy 160, high resolution spectra at pass energy 20. 3D micro CT data were acquired via the CTLab at the Australian National University (ANU) with a laboratory-based high resolution 3D X-ray computed tomography instrument developed by the Department of Applied Mathematics. Images were acquired at 60 keV and 50 mA, with a voxel size of 4.99 μm.

Electrochemical measurements

Electrochemical measurements of all the 3D current collector based electrodes are conducted in 2032-type coin cells. All 3D electrodes are prepared by sulfur-impregnation process. In comparison, the Al-foil based electrode is prepared by repeated drop-casting the cathode slurry onto Al foil round discs to reach a high sulfur mass loading level. The Al-foil based electrodes contains 70 wt.% sulfur (99.5%, Sigma

Aldrich), 20 wt.% SP carbon black nanoparticles (99.5%, MTI corp., USA), and 10 wt.% of polyvinylidene fluoride (PVDF, 99.5%, MTI Corp., USA) binder. All electrodes are dried overnight in an oven at 60 °C before further use. All cells are assembled in an argon-filled glovebox and use metallic lithium foils (99.9%, Sigma Aldrich) as the negative electrodes. The electrolyte contains 1 M lithium bis (trifluoromethanesulfonyl) imide (LiTFSI, 99.9%) and 0.1 M lithium nitrate ($LiNO_3$) in a mixture of DME and DOL (1:1, vol.). The average volume of electrolyte added in each cell is about 60 – 80 μL. Galvanostatic discharge/charge cycling and rate performance measurements are performed with a NEWARE Battery Testing System at room temperature. The electrochemical impedance spectroscopy (EIS) and cyclic voltammetry (CV) are carried out with a BioLogic VMP-3 Multi-channel Potentiostat workstation.

Calculation of volumetric capacity (C_V) and energy density (E_V)

The calculation of volumetric capacity (C_V) and energy density (E_V) of the 3D electrodes are conducted with the following method. The shape of the 3D electrodes can be approximated by a cylindrical shape, and computed as:

$$V_{3D} = S_{3D} \times H_{3D} = (\pi \cdot r_{3D}^2) \times H_{3D}, \quad [1]$$

where S_{3D}, H_{3D} and r_{3D} are the projected area, the thickness and radius of 3D electrode, respectively. Considering that the 3D electrode thickness, determined by SEM images, is within 120 – 140 μm. Here an approximate average value of H_{3D} = 130 μm and r_{3D} = 0.5 cm are employed for the computation of the electrode volume, resulting in a V_{3D} of 0.0102 cm^3.

The cathode density (ρ) can be estimated by:

$$\rho = (m_{3D} + m_{sulfur}) / V_{3D}, \quad [2]$$

where ρ is the cathode density, g cm^{-3}, m_{3D} is the mass of the 3D current collector, including the 3D carbon scaffold and the MOFs nanoparticles, g, m_{sulfur} is the mass of sulfur loaded, g, and V_{3D} is the volume of the cathode, cm^3.

The cathode's volumetric capacity (C_V) can be estimated from the areal capacity (C_A) by:

$$C_V = C_A / H_{3D}. \quad [3]$$

The cathode's volumetric energy density (E_V) can be estimated by:

$$E_V = \rho \cdot C \cdot U, \quad [4]$$

where ρ is the cathode density, g cm^{-3}, C is the gravimetric discharge capacity, mAh g^{-1}, and U is the approximate discharge plateau of the cathode, V (vs. Li^+/Li).

The volumetric capacities of the ZIF-67- and HKUST-1-based 3D MOF-carbon monoliths, listed in **Figure 4e,** are C_V = 1785 mAh cm^{-3} (0.05C) and 946 mAh cm^{-3} (0.6C) and C_V = 1992 mAh cm^{-3} (0.05C) and 785 mAh cm^{-3} (0.6C), respectively. Assuming the average operating voltage of the sulfur cathode to be 2.1 V (vs. Li^+/Li), the initial volumetric energy density ($E_{V\text{-}3D}$) of the ZIF-67- and HKUST-1-based electrodes are about 1946.7 Wh L^{-1} (0.6C) and 1615.4 Wh L^{-1} (0.6C), respectively. These are comparable to those of state-of-the-art cathode materials, such as $LiCoO_2$ and $Li(Ni_{1/3}Co_{1/3}Mn_{1/3})O_2$ of ~2000 Wh L^{-1} (1C).[S5] It should be noted that the volumetric capacity and energy density of a sulfur cathode cannot be directly compared to the aforementioned conventional cathode materials. As sulfur is in a quasi-liquid state and

undergo a volume variation of ~80% during the discharge and charge processes, the void space of the 3D electrodes are beneficial in accommodating this volume expansion. With respect to other Li-S electrodes, reporting values of 400 – 600 Wh L^{-1},[S6] our 3D electrode volumetric energy density is significantly higher.

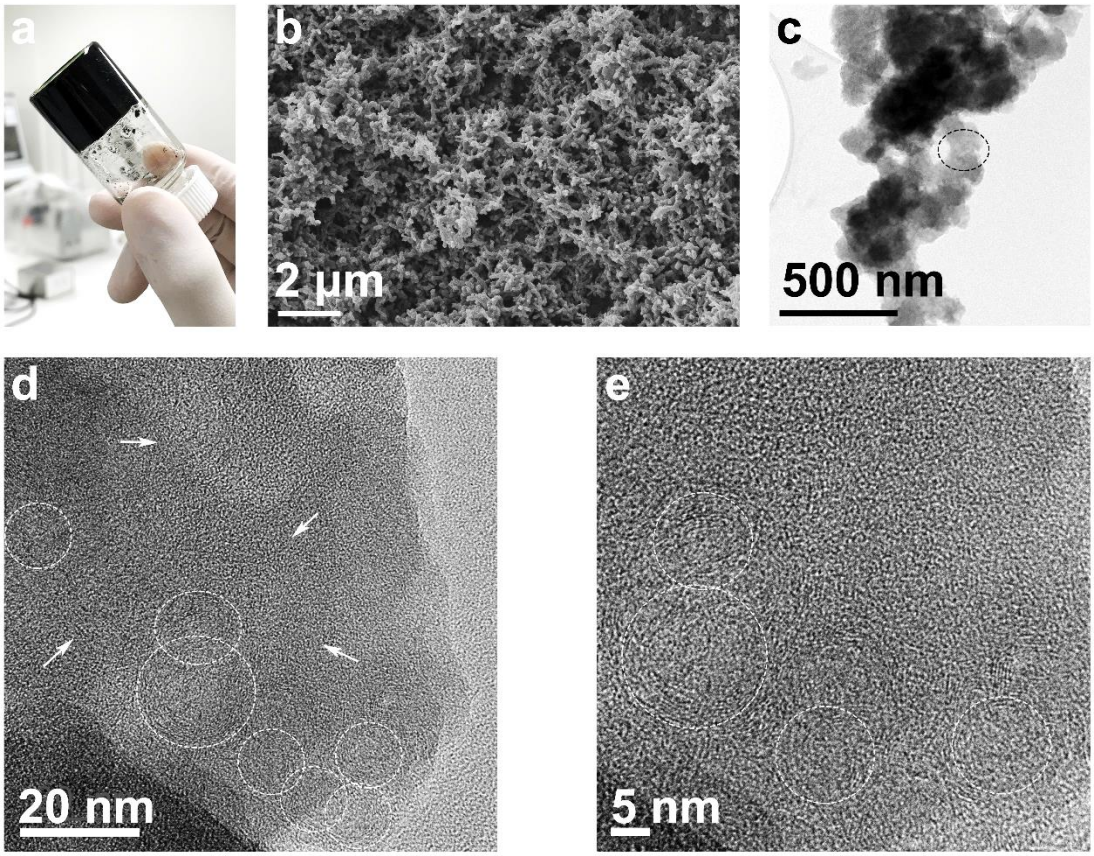

Figure S1 (a) Digital images of 3D SP@PANi CPH. (b) SEM images of 3D SP@PANi CPH. (c) TEM image of 3D SP@PANi CPH, where the black circle indicates the targeted area for HRTEM analysis. (d) High-magnification TEM image of 3D SP@PANi CPH, where the circles indicate the locations of SP nanoparticles with graphite-like lattice structures and the arrows indicate the areas of PANi hydrogel. (e) HRTEM image of 3D SP@PANi CPH, where the white circles indicate the locations of SP nanoparticles with graphite-like lattice structures.

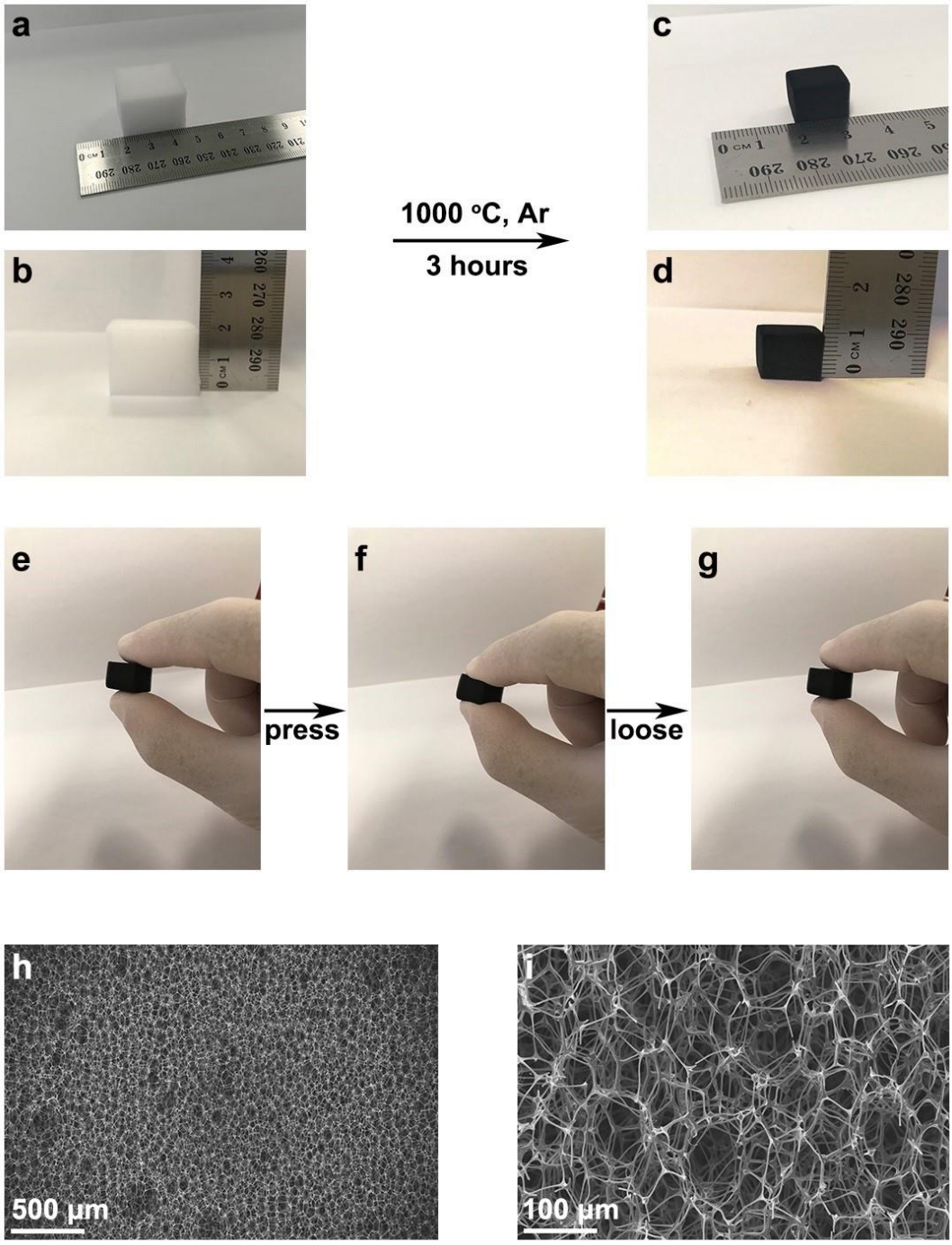

Figure S2 Schematic illustration of commercially available melamine foams (a,b) before and (c,d) after pyrolysis. No apparent morphology change has been observed after carbonization at 1000 °C for 3 hours under Ar flow protection. (e-g) The carbonized melamine foam can recover its shape after being hand-pressed without apparent structural failure, demonstrating its mechanical stability and elasticity maintenance even after pyrolysis. (h,i) SEM images of carbonized melamine foam.

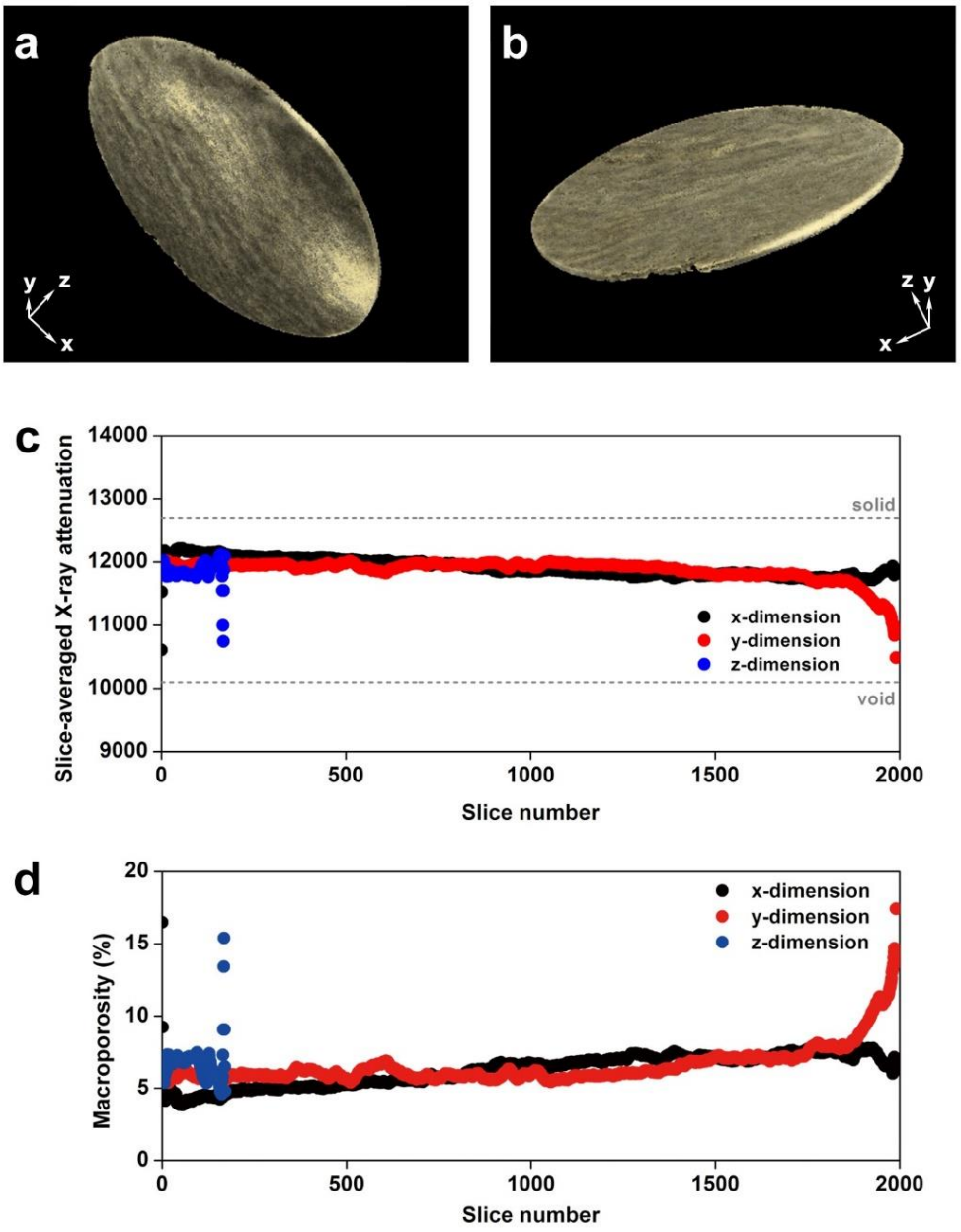

Figure S3 (a-b) 3D micro CT scanned model of a single piece of 3D CIMC current collector with two different viewing angles. (c) Slice-averaged X-ray attenuation of a single piece of 3D CIMC current collector on the x, y, and z dimensions. The dash lines signify void and solid pixels in the 3D CT greyscale model. (d) Calculated macro-porosity of 3D CIMC current collector. The sudden variations in the plots are due to edge-effect of the specimen.

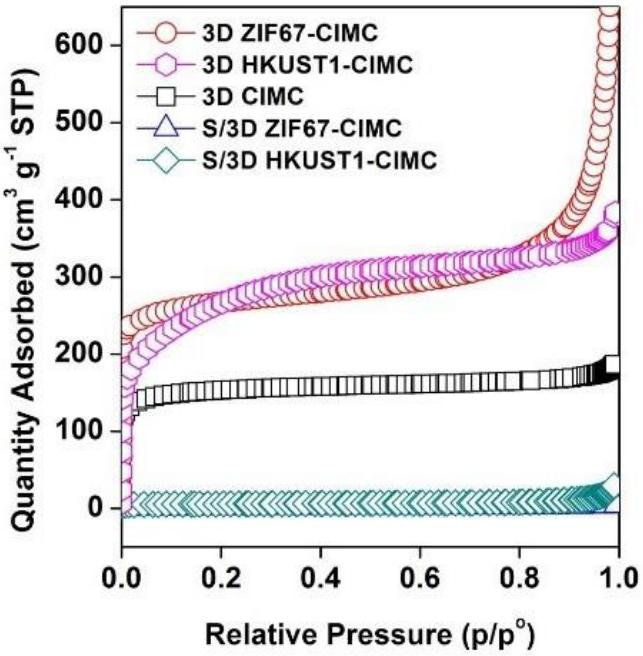

Figure S4 Brunauer–Emmett–Teller (BET) results of the 3D current collectors.

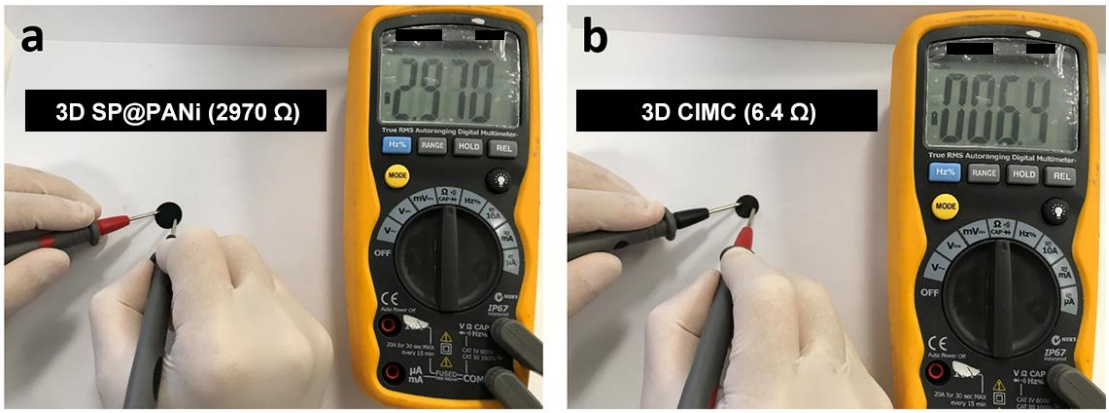

Figure S5 Qualitative resistance measurement using a multimedia for the free-standing (a) 3D SP@PANi CPH disc and (b) 3D CIMC current collector with high electrical conductivity.

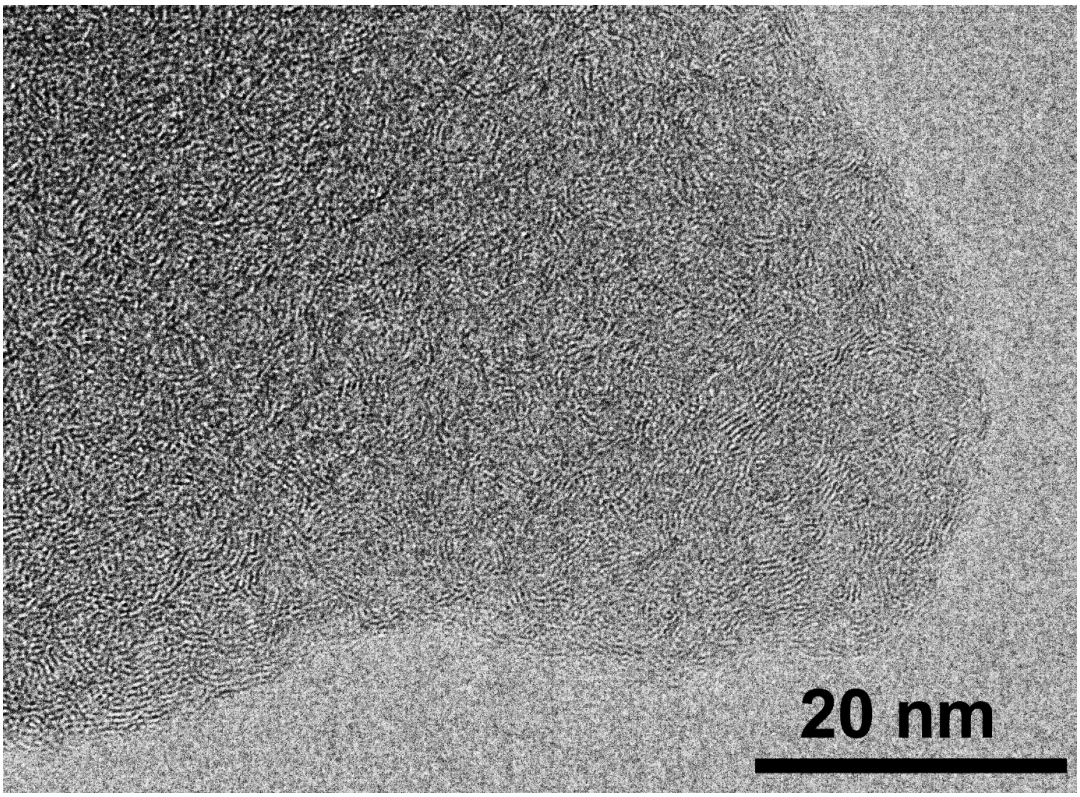

Figure S6 HRTEM image (in-plain focus) shows graphite-like domains in the 3D carbon network, corresponding to region#1 in Figure 1e.

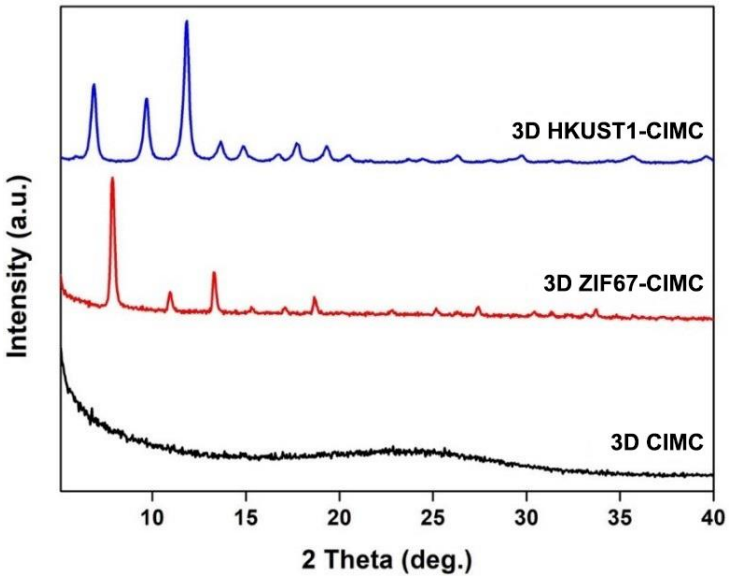

Figure S7 XRD patterns of 3D CIMC, 3D ZIF67-CIMC and 3D HKUST1-CIMC. The hump at about 25° is due to the partially graphitized amorphous carbon in the 3D CIMC. The major peaks of 3D ZIF67-CIMC and 3D HKUST1-CIMC are in good agreement with previous studies.[S6, S7]

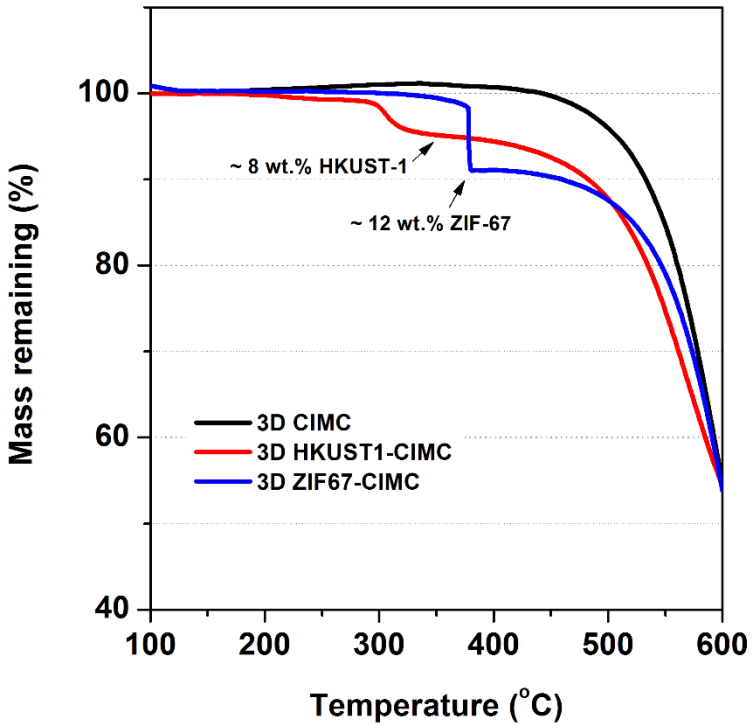

Figure S8 TGA curves of the 3D CIMC, and 3D ZIF67-CIMC and 3D HKUST1-CIMC hybrids. The calculation of the weight percentages of ZIF-67 MOF and HKUST-1 MOF were based on their products (CuO for HKUST-1, Co_3O_4 for ZIF-67) at the temperature pointed out by the arrows in the above figure. Parallelly, the results were also adjusted by weighing the samples before and after MOF-impregnation on an electronic balance.

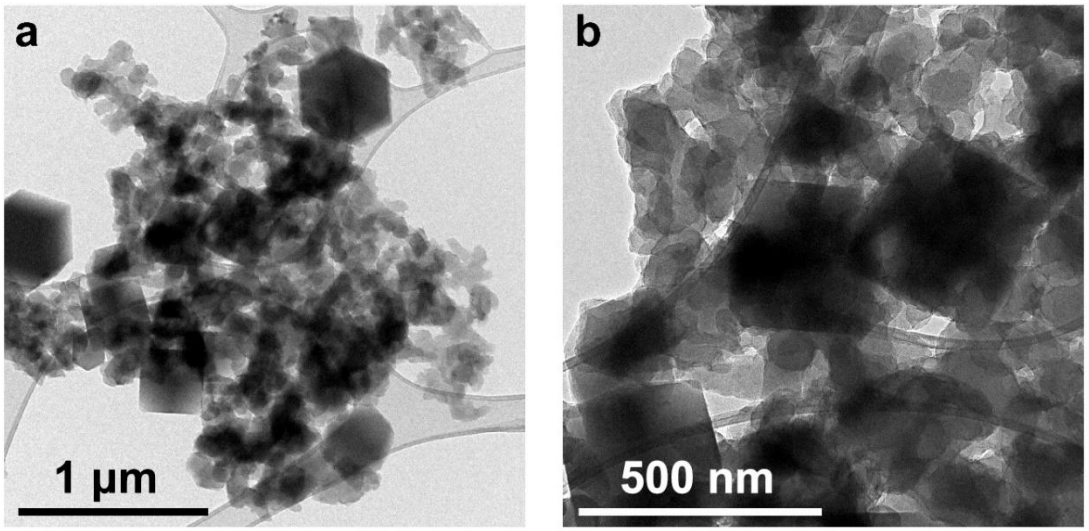

Figure S9 TEM images of 3D ZIF67-CIMC hybrid structure.

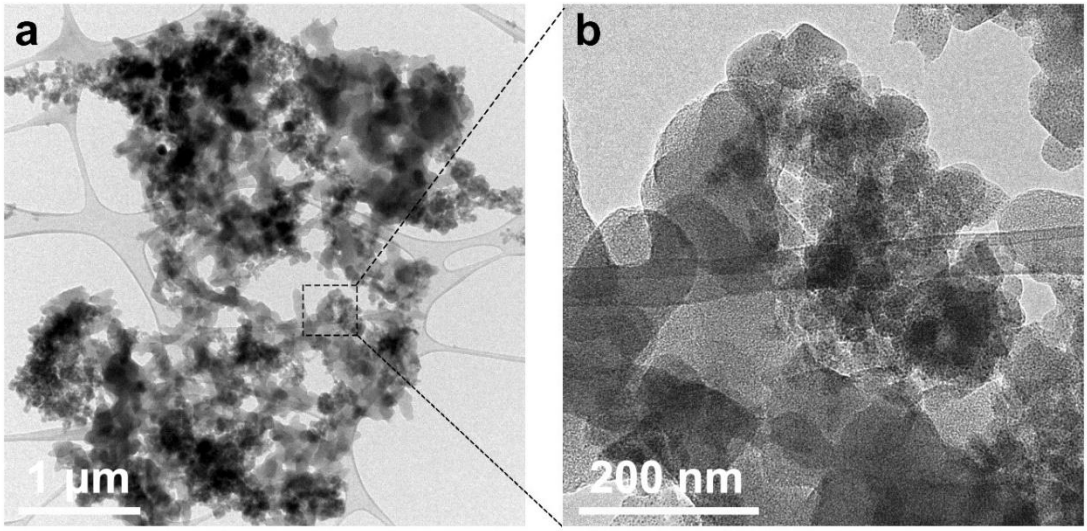

Figure S10 TEM images of 3D HKUST1-CIMC hybrid structure.

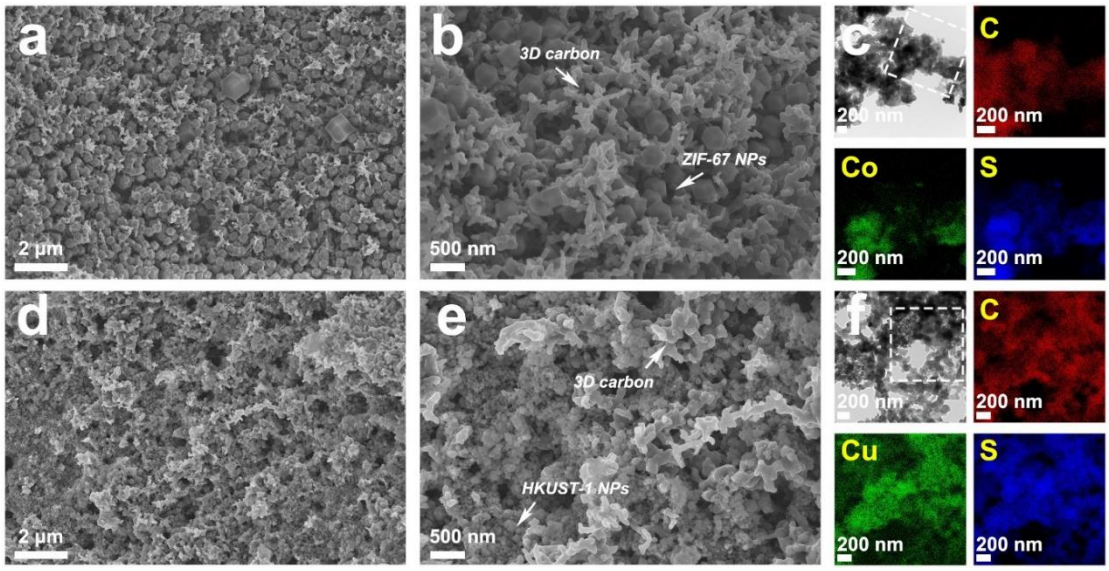

Figure S11 TEM images and EDX elemental mapping of the S-impregnated 3D MOF-carbon hybrid nanostructures. The S maps for both hybrid electrodes matches well with those of Co maps, indicating successful S-impregnation in MOF domains.

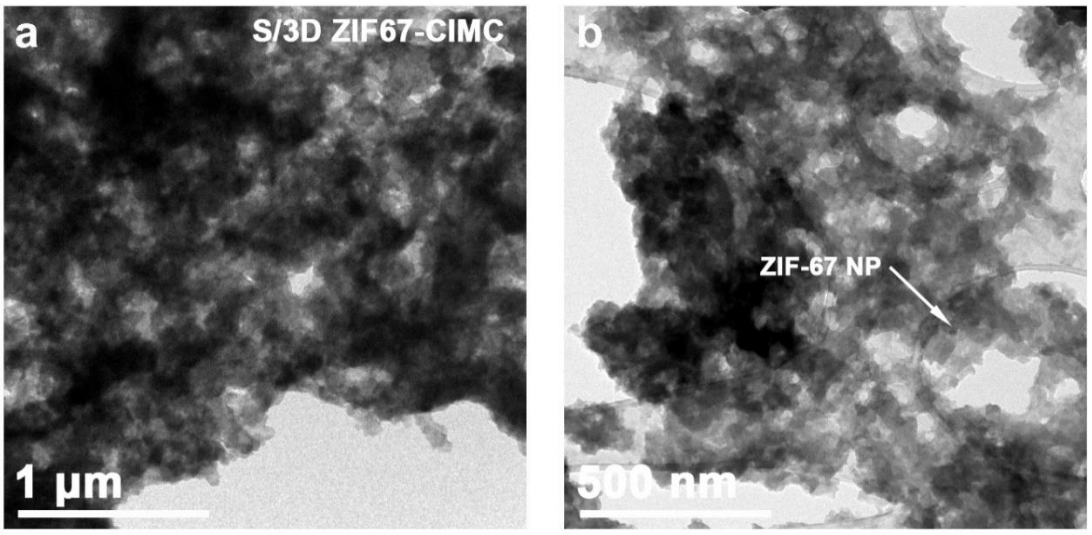

Figure S12 Higher magnification TEM images of S-impregnated 3D ZIF67-CIMC. Scale bars: 1 μm (a) and 500 nm (b). ZIF-67 nanoparticle is still able to be identified directly in the image or by EDX mapping, though the electrode structure was slightly destructed during sample preparation for TEM analysis.

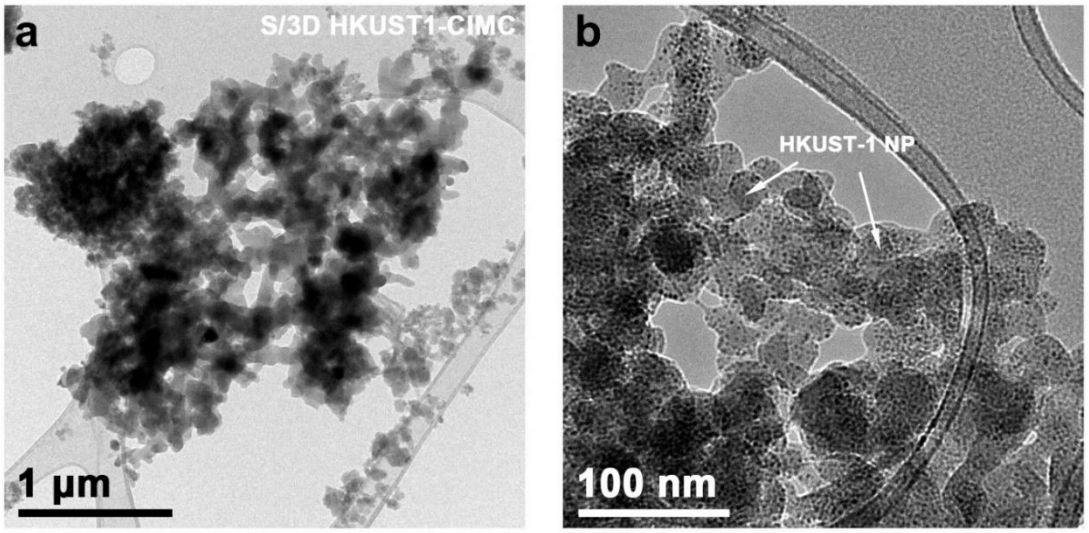

Figure S13 Higher magnification TEM images of S-impregnated 3D HKUST1-CIMC. Scale bars: 1 μm (a) and 100 nm (b).

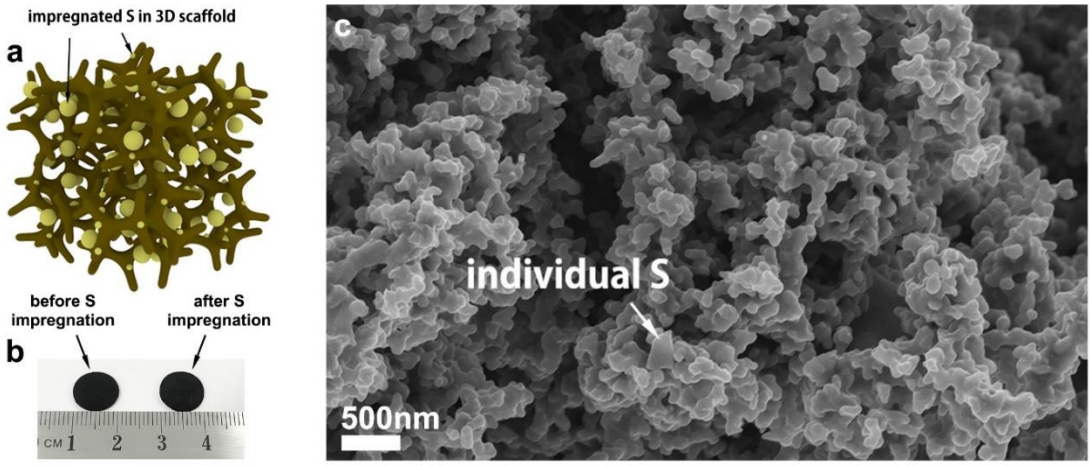

Figure S14 S-impregnated 3D carbon electrode (S/3D CIMC). (a) Schematic illustration of S/3D CIMC electrode. (b) No obvious color or structure change happened after S impregnation, indicating outstanding S impregnation in 3D CIMC. (c) SEM shows not much S aggregation of the S/3D CIMC electrode.

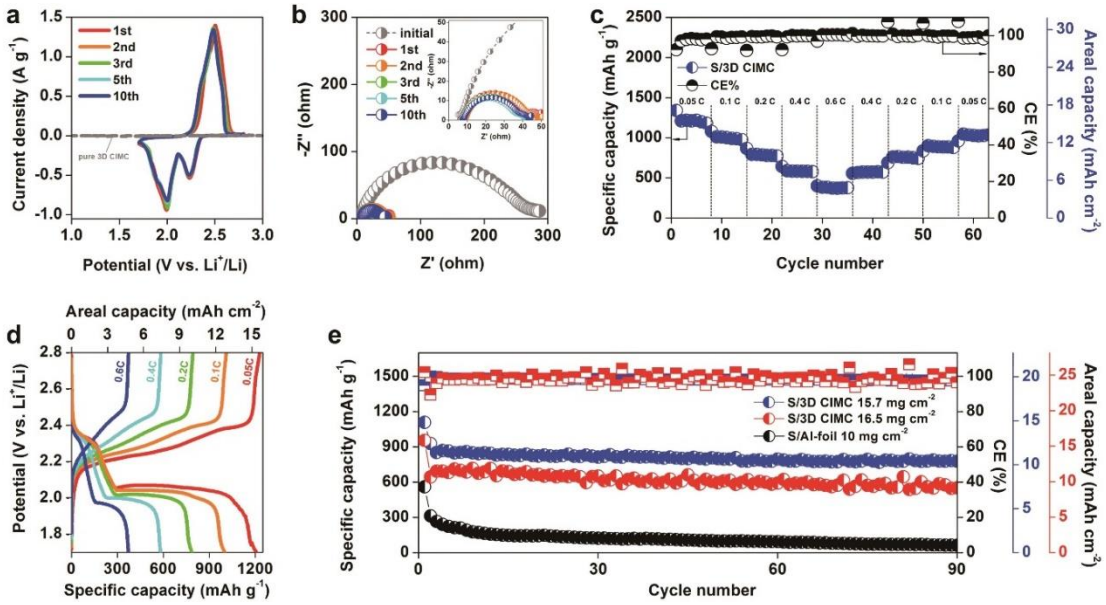

Figure S15 Electrochemical performance of the 3D carbon electrode. (a) CV plots of the S/3D CIMC at 0.1 mV s^{-1}. The grey dashed curves are attributed to pure 3D carbon current collector as a reference. (b) Nyquist plots of the S/3D CIMC electrode. Inset: A zoom-in view of the EIS spectrum. (c) Rate performance of the S/3D CIMC electrode from 0.05 - 0.6C with sulfur loading of ca. 10 mg cm^{-2}. (d) Discharge-charge profiles of the S/3D CIMC electrode from 1.7 V to 2.8 V. (e) Cycling performance of the S/3D CIMC electrode and Al-foil based electrode at 0.1C with S loading of ca. 10.5 mg cm^{-2} and ca. 13 mg cm^{-2}.

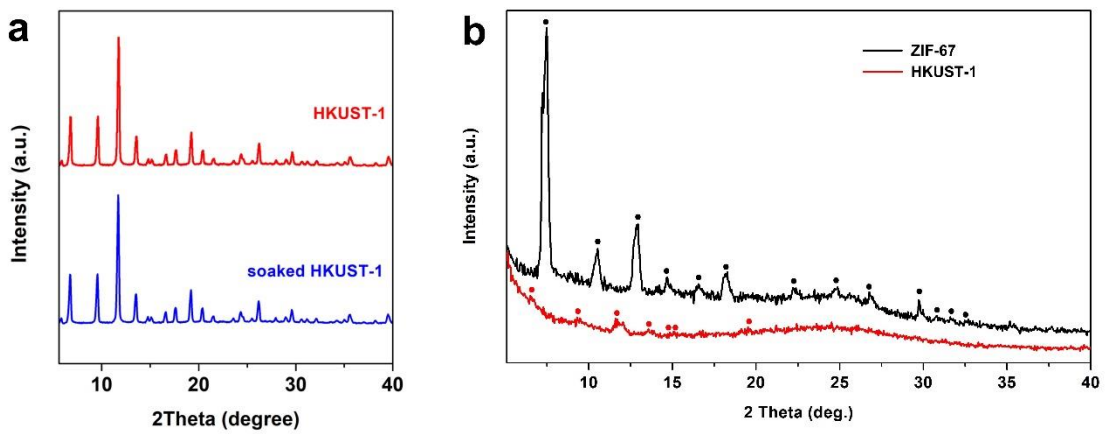

Figure S16 (a) XRD patterns of pure HKUST-1 particles before and after being soaked in the Li−S battery electrolyte. The particles were washed with ethanol for a couple of times after soaking. (b)XRD patterns of post-cycling 3D ZIF67-CIMC and 3D HKUST1-CIMC electrodes (discharged state). The electrodes have been rinsed with electrolyte for at least 5 times and dried naturally in an Ar-filled glovebox. Main characteristic peaks of ZIF-67 MOF and HKUST-1 MOF are highlighted with black and white dots in the above figure, respectively, confirming their existence after cycling. The weakened peak intensity of post-cycling MOFs could be due to the existence of impurities left in the electrodes.

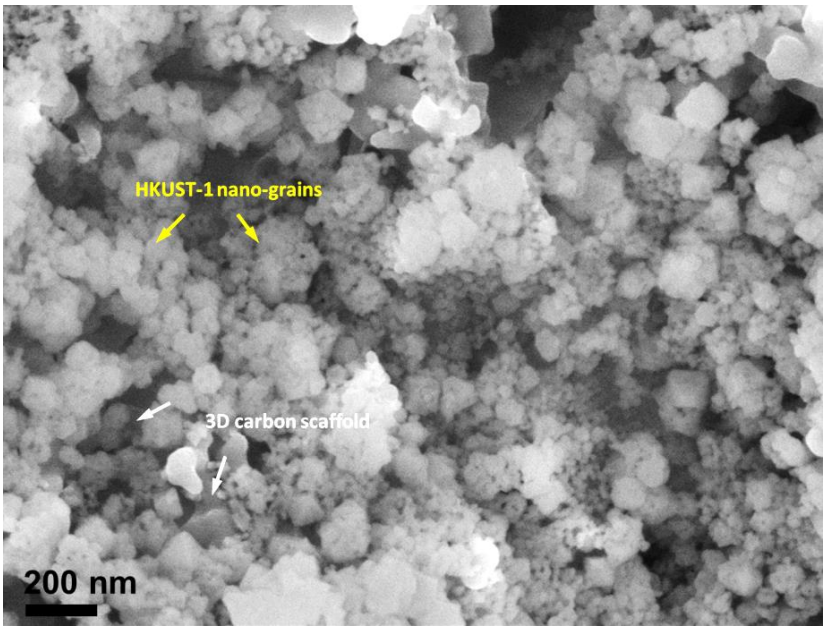

Figure S17. SEM image of the post-cycling 3D electrodes with HKUST-1 domains.

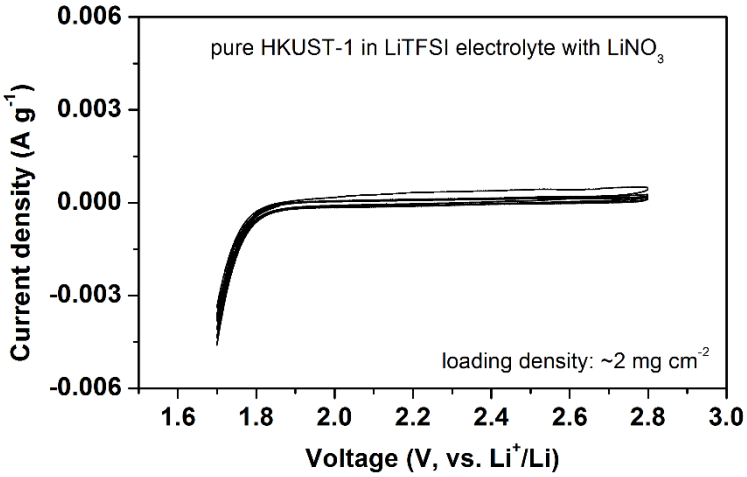

Figure S18. CV curves of pure HKUST-1 cathodes in the LiTFSI electrolyte. The cathodes are composed of 60 wt.% HKUST-1 (~2mg cm^{-2}) with 30 wt.% SuperP and 10 wt.% PVDF binder on Al foils. The SuperP carbon black is to ensure the electrons can be transferred to HKUST-1. The results indicate no obvious redox reaction from Cu^{2+}/Cu^{+} in the operation voltage range of Li−S batteries.

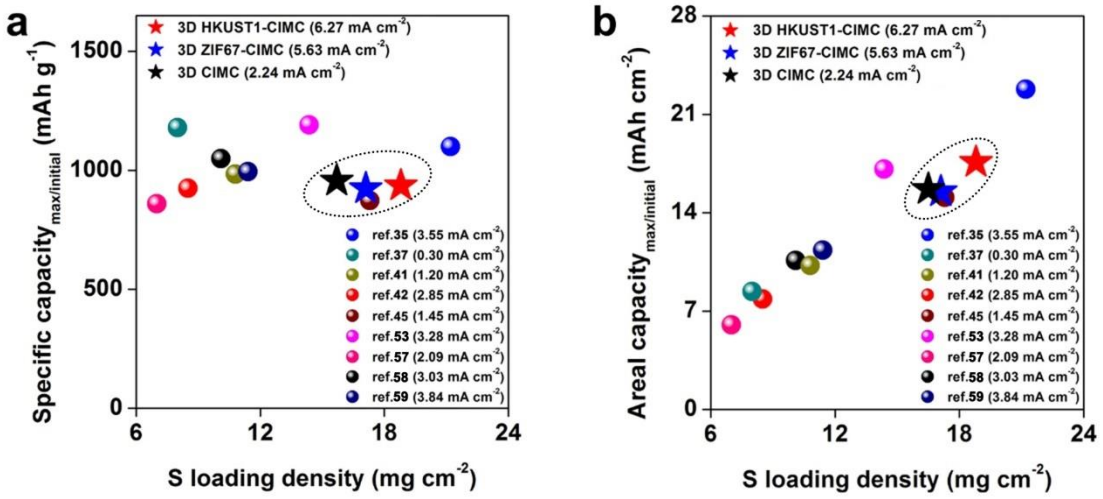

Figure S19 Comparison of (a) specific capacity and (b) areal capacity of our 3D electrodes with those of Li–S batteries from recent studies with sulfur loading densities higher than 6 mg cm^{-2}.

References

S1. Pan, L.; Yu, G.; Zhai, D.; Lee, H. R.; Zhao, W.; Liu, N.; Wang, H.; Tee, B. C.-K.; Shi, Y.; Cui, Y. *Proceedings of the National Academy of Sciences* **2012,** 109, (24), 9287-9292.

S2. Liu, B.; Soares, P.; Checkles, C.; Zhao, Y.; Yu, G. *Nano Letters* **2013,** 13, (7), 3414-3419.

S3. Shi, Y.; Pan, L.; Liu, B.; Wang, Y.; Cui, Y.; Bao, Z.; Yu, G. *Journal of Materials Chemistry A* **2014,** 2, (17), 6086-6091.

S4. Xue, W.; Miao, L.; Qie, L.; Wang, C.; Li, S.; Wang, J.; Li, J. *Current Opinion in Electrochemistry* **2017,** 6, (1), 92-99.

S5. Shaju, K. M.; Bruce, P. G. *Advanced Materials* **2006,** 18, (17), 2330-2334.

S6. Mao, Y.; Li, G.; Guo, Y.; Li, Z.; Liang, C.; Peng, X.; Lin, Z. *Nature Communications* **2017,** 8, 14628.

S7. Chen, Y. Z.; Wang, C.; Wu, Z. Y.; Xiong, Y.; Xu, Q.; Yu, S. H.; Jiang, H. L. *Advanced Materials* **2015,** 27, (34), 5010-5016.